

The MAP Kinase MPK4 Is Required for Cytokinesis in *Arabidopsis thaliana* ^W

Ken Kosetsu,^a Sachihiko Matsunaga,^b Hirofumi Nakagami,^{c,1} Jean Colcombet,^d Michiko Sasabe,^a Takashi Soyano,^{a,2} Yuji Takahashi,^a Heribert Hirt,^{c,d} and Yasunori Machida^{a,3}

^a Division of Biological Science, Graduate School of Science, Nagoya University, Chikusa-ku, Nagoya 464-8602, Japan

^b Department of Biotechnology, Graduate School of Engineering, Osaka University, Suita, Osaka 565-0871, Japan

^c Department of Plant Molecular Biology, Max F. Perutz Laboratories, University of Vienna, A-1030 Vienna, Austria

^d Unité de Recherche en Génomique Végétale Plant Genomics, Institut National de la Recherche Agronomique, Centre National de la Recherche Scientifique, Université d'Evry, 91057 Evry, France

Cytokinesis in plants is achieved by the formation of the cell plate. A pathway that includes mitogen-activated protein (MAP) kinase kinase kinase and MAP kinase kinase (MAPKK) plays a key role in the control of plant cytokinesis. We show here that a MAP kinase, MPK4, is required for the formation of the cell plate in *Arabidopsis thaliana*. Single mutations in *MPK4* caused dwarfism and characteristic defects in cytokinesis, such as immature cell plates, which became much more prominent upon introduction of a mutation in *MKK6/ANQ*, the MAPKK for cytokinesis, into *mpk4*. *MKK6/ANQ* strongly activated MPK4 in protoplasts, and kinase activity of MPK4 was detected in wild-type tissues that contained dividing cells but not in *mkk6/anq* mutants. Fluorescent protein-fused MPK4 localized to the expanding cell plates in cells of root tips. Expansion of the cell plates in *mpk4* root tips appeared to be retarded. The level of *MPK11* transcripts was markedly elevated in *mpk4* plants, and defects in the *mpk4 mpk11* double mutant with respect to growth and cytokinesis were more severe than in the corresponding single mutants. These results indicate that MPK4 is the downstream target of *MKK6/ANQ* in the regulation of cytokinesis in *Arabidopsis* and that MPK11 is also involved in cytokinesis.

INTRODUCTION

Cytokinesis is an essential feature of the life cycle of all cellular organisms, since it is the process whereby duplicated chromosomes and cytoplasm are distributed to daughter cells during cell division. This partitioning must be temporally and spatially controlled, but details of the mechanism that controls it remain unknown. At least two morphologically distinct processes result in cytokinesis: (1) the outside-in formation of cleavage furrows via constriction of an actomyosin-based contractile ring and/or septum and the functions of a microtubule (MT)-based midbody, which is found in yeast and animal cells (reviewed in Pollard, 2010); and (2) the formation of a septum (the cell plate) in the inside-out direction that is mediated by the centrifugal expansion of the phragmoplast, which consists of MTs and is found in higher plants (reviewed in Jürgens, 2005; Sasabe and Machida, 2006).

In plants, the phragmoplast forms between two separating daughter nuclei during anaphase of the cell cycle, consists mainly

of specific and complex arrays of MTs and microfilaments, and expands centrifugally toward the parental cell wall. The expansion of the phragmoplast occurs via the turnover of MTs, which includes the polymerization of tubulins at the outer periphery of the equatorial region of the phragmoplast and the depolymerization of MTs in the inner region of the equatorial plane (Asada et al., 1991; Hush et al., 1994; reviewed in Nishihama and Machida, 2001). Vesicles derived from Golgi bodies accumulate and fuse in the equatorial region (Samuels et al., 1995; Reichardt et al., 2007). It has been proposed that cell walls are generated in such vesicles (reviewed in Verma, 2001; Mayer and Jürgens, 2004). A number of Rab-GTPases and some regulators and effectors of these enzymes have been shown to be involved in the membrane trafficking that occurs during plant cytokinesis (reviewed in Woollard and Moore, 2008). It is clear that the turnover of MT arrays in the phragmoplast, the fusion of vesicles, and the generation of cell walls and cell membranes must be controlled and coordinated during the progression of cytokinesis and the formation of the cell plate (Yasuhara et al., 1995; Gu and Verma, 1996; Yasuhara and Shibaoka, 2000; Zuo et al., 2000; reviewed in Jürgens, 2005).

The components of the NACK-PQR pathway, identified in tobacco (*Nicotiana tabacum*) BY-2 cultured cells, are key regulators of plant cytokinesis, and they include a mitogen-activated protein (MAP) kinase cascade and NACK kinesin-like proteins, which function as activators of the cascade (Nishihama et al., 2001, 2002; Ishikawa et al., 2002; Soyano et al., 2003). The MAPK cascade consists of NPK1 MAP kinase kinase kinase (MAPKKK) (Banno et al., 1993), NQK1/MEK1 MAP kinase kinase (MAPKK),

¹ Current address: RIKEN Plant Science Center, 1-7-22 Suehiro-cho, Tsurumi, Yokohama 230-0045, Japan.

² Current address: National Institute of Agrobiological Sciences, Kannon-dai, Tsukuba, Ibaraki 305-8602, Japan.

³ Address correspondence to yas@bio.nagoya-u.ac.jp.

The author responsible for distribution of materials integral to the findings presented in this article in accordance with the policy described in the Instructions for Authors (www.plantcell.org) is: Yasunori Machida (yas@bio.nagoya-u.ac.jp).

^W Online version contains Web-only data.
www.plantcell.org/cgi/doi/10.1105/tpc.110.077164

and NRK1/NTF6 MAP kinase (MAPK) (Soyano et al., 2003). Two M-phase-specific kinesin-like proteins in tobacco, designated NACK1 and NACK2, activate NPK1 via direct interaction with NPK1, and interference with this interaction in BY-2 cells results in typical defects in cytokinesis, suggesting a requirement for both NACK1 and NPK1 in cytokinesis (Nishihama et al., 2001, 2002; Ishikawa et al., 2002). The protein kinases NPK1 MAPKKK and NQK1 MAPKK are activated during the late M-phase, and expression of kinase-negative NQK1 MAPKK also results in defects in cytokinesis in BY-2 cells, suggesting an essential role for NQK1 downstream of NPK1 MAPKKK in cytokinesis (Soyano et al., 2003).

The activity of NRK1/NTF6 MAPK also increases in parallel with the activities of NPK1 and NQK1 at the late M-phase in tobacco BY-2 cells (Soyano et al., 2003). The NRK1 protein associates physically with NQK1 MAPKK and is activated by NQK1. Activated NRK1 MAPK phosphorylates the MT-associated protein MAP65-1 of tobacco both in vitro and in vivo (Sasabe et al., 2006). Phosphorylation of MAP65-1 decreases the ability of MAP65-1 to bundle MTs in vitro and, in this way, might stimulate depolymerization of MTs and enhance the expansion of the phragmoplast in vivo. In addition, NRK1/NTF6, the homolog of NTF6 in alfalfa (*Medicago sativa*), and the phosphorylated forms of the MAP65 proteins are concentrated at the equator of the phragmoplast in tobacco cells (Calderini et al., 1998; Bögre et al., 1999; Sasabe et al., 2006), an observation consistent with the roles of these MAPKs and MAP65 in the turnover of MTs in vivo. Conversely, the addition of an MT-depolymerizing reagent, such as propyzamide, to BY-2 cells with expanding phragmoplasts induces the rapid inactivation of three kinases, NPK1 MAPKKK, NQK1 MAPKK, and NRK1 MAPK, as well as the depolymerization of MTs (Soyano et al., 2003; reviewed in Jürgens, 2005). Taken together, the various observations suggest that NRK1 might control the formation of the cell plate by modulating the function of MAP65 in the equatorial region of the phragmoplast. In animal cells, ERK1/2 MAPKs are localized in the spindle midzone and midbody (Shapiro et al., 1998; Zecevic et al., 1998; Kasahara et al., 2007). The inhibition of MEK1/2 MAPKKs, which act upstream of ERK1, by U0126, an inhibitor of MEKs, leads to abscission failure in HeLa cells (Kasahara et al., 2007). These observations support the hypothesis that the ERK1 MAPK might also regulate cytokinesis in animal cells. In spite of the accumulation of considerable circumstantial evidence, the involvement of MAPKs in cytokinesis in all organisms remains incompletely proven because of the absence of appropriate genetic evidence.

To gain a deeper understanding of the role of the NACK-PQR pathway in cytokinesis, we exploited molecular and genetic approaches in the model plant *Arabidopsis thaliana*. Most of components of the NACK-PQR pathway of *Arabidopsis* have been identified. *HINKEL/NACK1* and *STUD/TETRASPORE/NACK2* are orthologs of tobacco *NACK1* and *NACK2*, respectively (Nishihama et al., 2002; Strompen et al., 2002; Yang et al., 2003; Tanaka et al., 2004). The *ANP1*, *ANP2*, and *ANP3* genes are, all three, orthologs of the *NPK1* gene for a MAPKKK of tobacco (Nishihama et al., 1997; Krysan et al., 2002), and the *MKK6/ANQ* gene for a MAPKK is an ortholog of tobacco *NQK1* and functions in cytokinesis (Soyano et al., 2003). *Arabidopsis* has 20 MAPK

homologs (reviewed in Ichimura et al., 2002), and some of these likely regulate cytokinesis.

The 20 MAPKs of *Arabidopsis* have been classified into four subfamilies, and five members of the group B subfamily, namely, MPK4, MPK5, MPK11, MPK12, and MPK13, are most similar, in terms of their amino acid sequences, to NRK1/NTF6 MAPK of tobacco. We report here that MPK4 is a crucial regulator of cytokinesis and that MPK11 is also involved in this regulation. In addition, our results show that levels of *MPK11* transcripts rise markedly in *mpk4* mutant plants, suggesting the negative regulation of *MPK11* transcription by MPK4.

RESULTS

The *mpk4-1* and *mpk4-2* Alleles, on the Columbia-0 Background, Cause Defects in the Formation of the Cell Plate

The *mpk4-2* allele on the Columbia-0 (Col-0) background (SALK_056245) corresponds to the *MPK4* gene with a T-DNA insert in the sixth exon (Figure 1E). The plant with this allele has been reported to be a null mutant (Xing et al., 2008). In our laboratory, the *mpk4-2* mutant that was provided by the stock center was backcrossed with the wild-type plant (Col-0) three times, and progeny plants were used in these experiments. A wild-type phenotype was restored by a transgene that contained the *MPK4* genomic region (see Supplemental Figure 1 online). As described below (Figure 1F; see Supplemental Figure 6 online), we failed to detect the *MPK4* transcript and MPK4 protein in the *mpk4-2* mutant, an observation consistent with the previously reported observation (Xing et al., 2008). Homozygous *mpk4-2* mutant plants exhibited severe aboveground dwarfism (Figures 1A and 1C), retarded root growth (Figure 1C), and the protrusion of many epidermal cells from roots (Figures 1G and 1I). The *mpk4-2* homozygous mutant set only a few flowers, and these flowers produced very few viable seeds or none at all. The roots (Figures 1K and 1M) and cotyledons (Figures 1O, 1P, 1S, and 1T) of the *mpk4-2* mutant contained enlarged cells with incomplete cell walls and multiple nuclei, as also observed previously in the *mkk6-1/anq-1* MAPKK mutant (Soyano et al., 2003). These results suggested that formation of the cell plate was severely impaired in dividing cells of the *mpk4-2* mutant.

In this study, the *mpk4-1* mutation on the Landsberg *erecta* (*Ler*) background was the result of an insertion of a *Ds* transposon in the first intron of the *MPK4* gene (Figure 1E; Petersen et al., 2000). Although *mpk4-1* plants also exhibited aboveground dwarfism, consistent with a previous observation (Petersen et al., 2000), the roots were relatively normal (Figures 1B and 1H), and no obvious cytokinetic defects were detected in cotyledons and roots (Figures 1L, 1Q, and 1R). We examined the splicing of the *Ds*-containing intron sequence in mRNA from this mutant by RT-PCR using a pair of primers that extended from the first exon to the second exon. We detected a transcript of the normal wild-type size, but the level of the transcript was very much lower than in the wild type (Figure 1F). Analysis of the nucleotide sequence of the transcript revealed that the first intron plus *Ds* had been appropriately excised in *mpk4-1* plants. Thus, this allele seems to

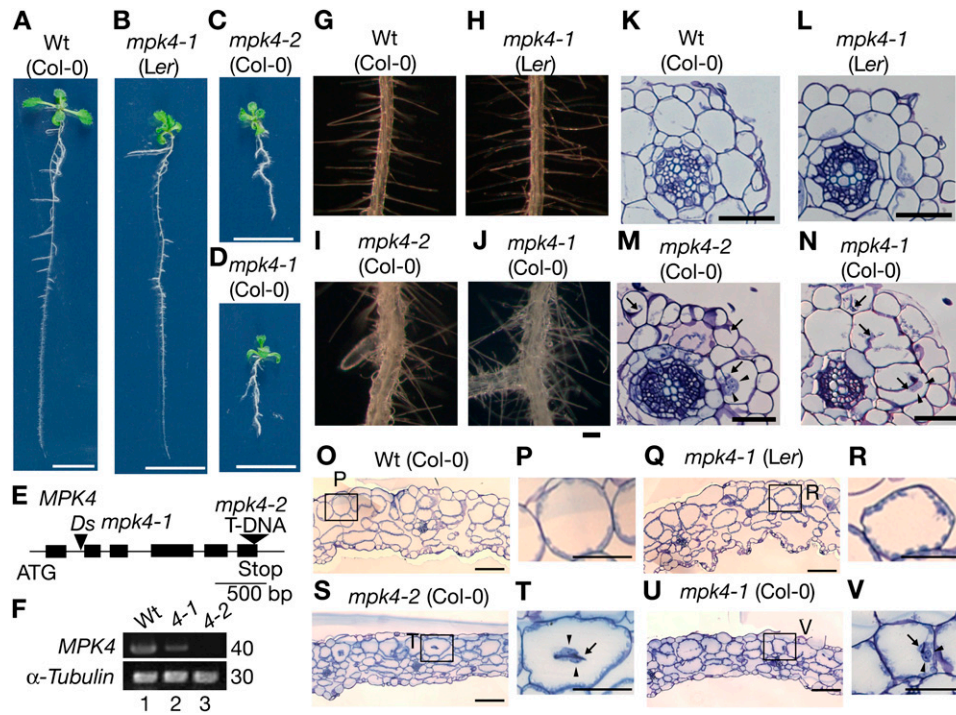


Figure 1. Effects of *mpk4* Alleles on the Growth and Organ Morphology of *Arabidopsis* and on Cell Division in Two Different Ecotypes, Col-0 and Ler. **(A)** to **(D)** Gross morphology of wild-type (Wt; Col-0; **[A]**), *mpk4-1* (Ler; **[B]**), *mpk4-2* (Col-0; **[C]**), and *mpk4-1* (Col-0; **[D]**) plants (12-d-old plants). Bars = 1 cm. **(E)** Sites of *Ds* transposon and T-DNA insertions in the alleles. **(F)** Analysis of transcripts. RT-PCR was performed with total RNA prepared from wild-type (Col-0; lane 1), *mpk4-1* (lane 2), and *mpk4-2* (lane 3) plants with primer pairs specific for the indicated genes. The number of cycles of PCR is indicated at the right of each panel. **(G)** to **(J)** Dark-field views of roots of wild-type (Col-0; **[G]**), *mpk4-1* (Ler; **[H]**), *mpk4-2* (Col-0; **[I]**), and *mpk4-1* (Col-0; **[J]**) plants. Bars = 0.25 mm. **(K)** to **(V)** Transverse sections of roots (**[K]** to **[N]**) and cotyledons (**[O]** to **[V]**) of 14-d-old plants stained with toluidine blue. Sections of the roots of wild-type (Col-0; **[K]**), *mpk4-1* (Ler; **[L]**), *mpk4-2* (Col-0; **[M]**), and *mpk4-1* (Col-0; **[N]**) plants. Bars = 50 μ m. Transverse sections of the cotyledons of wild-type (Col-0; **[O]**), *mpk4-1* (Ler; **[Q]**), *mpk4-2* (Col-0; **[S]**), and *mpk4-1* (Col-0; **[U]**) plants. Magnified views of boxed regions are shown in **(P)**, **(R)**, **(T)**, and **(V)**. Arrowheads and arrows in panels indicate nuclei in multinucleate cells and incomplete cross walls, respectively. Bars = 100 μ m in **(O)**, **(Q)**, **(S)**, and **(U)** and 50 μ m in **(P)**, **(R)**, **(T)**, and **(V)**.

correspond to a weak mutation. By contrast, no corresponding band was detected in the analysis of the RNA from *mpk4-2* plants under the same conditions, suggesting that the *mpk4-2* mutation has a stronger effect than *mpk4-1*, an observation consistent with the phenotypic difference noted above.

Since the *mpk4-2* allele was on the Col-0 background, we transferred the *mpk4-1* allele from the Ler background to the Col-0 background by outcrossing, and then we examined the resultant phenotypes. Figure 1D shows that the *mpk4-1* allele on the Col-0 background resulted in more severe dwarfism than the same allele on the Ler background. The protrusion of root epidermal cells was also evident in the *mpk4-1* plants as well as in the *mpk4-2* plants with the Col-0 background (Figures 1I and 1J), even though no such protrusions were observed in the case of *mpk4-1* roots with the Ler background (Figure 1H). To date, protrusions of this type have always been associated with defects in cytokinesis in mutants such as *mkk6-1/anq-1* and *hinkel/nack1* (Soyano et al., 2003). Examination of cross sections revealed that roots (Figure 1N) and cotyledons (Figures 1U and

1V) of *mpk4-1* (Col-0) plants contained unusually large cells with incomplete cell walls and multiple nuclei. By contrast, cells of *mpk4-1* (Ler) did not exhibit such abnormalities.

The Genetic Interaction between *mpk4-2* and *anq-2*

Phenotypic analysis of double mutants demonstrated that *mpk4-2 anq-2* exhibited more severe dwarfism than either single mutant (Figures 2A to 2D), confirming a role for *MPK4* in cytokinesis. To examine the genetic interaction between *mpk4-2* and *anq-2* in more detail, we generated *mpk4-2/+ anq-2/+* double heterozygotes and determined the genotypes of 197 self-pollinated progeny by examining the presence or the absence of the T-DNA that caused each respective mutation. As shown in Supplemental Table 1 online, the segregation ratios of the genotypes of the progeny deviated from the expected Mendelian frequencies. Segregation efficiencies of the genotypes *MPK4/+ anq-2/-* (line 3), *mpk4-2/+ anq-2/-* (line 6), and *mpk4-2/- anq-2/-* (line 9) were markedly lower than the expected values (see

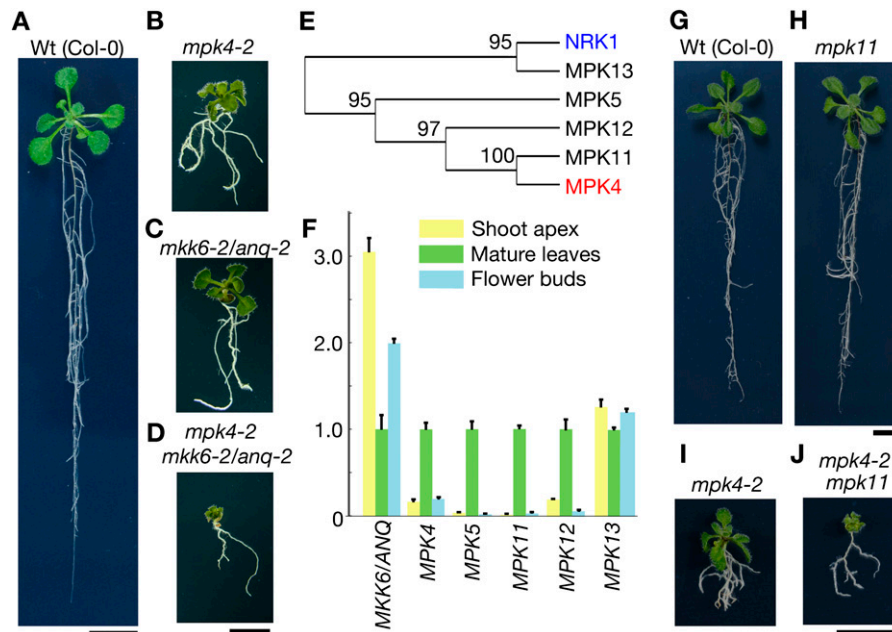


Figure 2. Comparison of the Phenotypes of the *mpk4-2 mkk6-2/anq-2* and *mpk4-2 mpk11* Double Mutants with That of Each Respective Single Mutant.

(A) to (D) Gross morphology of wild-type (Wt; Col-0) (A), *mpk4-2* (B), *mkk6-2/anq-2* (C), and *mpk4-2 mkk6-2/anq-2* (D) plants (15-d-old plants). All plants shown here had the Col-0 background. Plants were grown on MS basic medium. Bars = 0.5 cm.

(E) Phylogenetic tree for tobacco NRK1 and five MPKs in the group B subfamily. Amino acid sequences of tobacco NRK1 and group B subfamily MAPKs were aligned with the ClustalX program, and the resulting alignment was used to generate a phylogenetic tree with GENETYX-Mac version 13. Values indicate the number of times that each branch topology was found during bootstrap analysis.

(F) Accumulation of transcripts of MKK6/ANQ MAPK and five genes for MPKs in the indicated organs of the wild-type plant, as determined by real-time RT-PCR with primers specific for each respective gene. Quantitative RT-PCR data were normalized by reference to expression of the gene for β -tubulin, and values relative to that for mature leaves are shown. Error bars indicate SD ($n = 3$).

(G) to (J) Gross morphology of wild-type (G), *mpk11* (H), *mpk4-2* (I), and *mpk4-2 mpk11* (J) plants (17-d-old plants). All plants shown here had the Col-0 background. Plants were grown on MS basic medium. Bars = 1 cm.

expected 1). In particular, the reduction in frequency of *mpk4-2/+ anq-2/-* (line 6) and *mpk4-2/- anq-2/-* (line 9) was greater than the reduction in frequency of *MPK4/+ anq-2/-* plants (line 3). These results showed that both the *mpk4-2* and the *anq-2* mutations negatively affected some or all of the following: the formation of gametes in the parent, fertilization, and the viability of progeny plants.

To examine the viability of *mpk4-2 anq-2* gametes, we performed reciprocal crosses between an *mpk4-2/+ anq-2/+* double heterozygote and a wild-type parent (Table 1). When we used mutant pollen from the *mpk4-2/+ anq-2/+* parent for crosses with a wild-type female parent, mutant alleles were transmitted to ~50% of the offspring, as expected (Table 1), indicating that male gametophytes were viable. However, when we used pollen from the wild-type parent for crosses with the *mpk4-2/+ anq-2/+* female parent, the mutant alleles *mpk4-2*, *anq-2*, or *mpk4-2* plus *anq-2* were transmitted to the offspring at much lower than expected frequencies (Table 1). We found that 7% of female gametophytes and/or embryos that harbored *mpk4-2*, 66% of those that harbored *anq-2*, and 89% of those that harbored both *mpk4-2* and *anq-2* were not viable. The lower segregation efficiencies of mutants with the *anq-2/-*, *mpk4-2/+ anq-2/-*, and

mpk4-2 anq-2 alleles that are shown in Supplemental Table 1 online can be predicted from the viabilities summarized in Table 1.

Double Mutant *mpk4-2 mpk11* Plants Exhibited More Severe Dwarfism Than *mpk4-2* Plants

To investigate the possible involvement in cytokinesis of other MAPKs in group B, we analyzed the expression of the *MPK4*, *MPK5*, *MPK11*, *MPK12*, *MPK13*, and *MKK6/ANQ* genes in wild-type plants as well as the phenotypes of the single mutants *mpk11* and *mpk13* and the double mutants *mpk4 mpk11* and *mpk4 mpk13*. We prepared poly(A)⁺ RNAs from shoot apices, mature leaves, and flower buds of wild-type plants and quantified the transcripts of the various MAPK genes by real-time RT-PCR (Figure 2F). Levels of *MPK13* transcripts in shoot apices, flower buds, and mature leaves did not differ significantly. Transcripts of other MAPK genes, including *MPK4*, were detected in tissues that contained dividing cells, but their levels were higher in mature leaves than in tissues with dividing cells (Figure 2F).

In this study, the *mpk11* mutant (Col-0 background) was backcrossed with the wild type (Col-0), and the *mpk13* mutant

Table 1. Results of Reciprocal Crosses between the *mpk4-2/+ anq-2/+* Mutant and Wild-Type Plants

Cross	Gamete Frequency				P Value
	<i>MPK4 ANQ</i>	<i>mpk4-2 ANQ</i>	<i>MPK4 anq-2</i>	<i>mpk4-2 anq-2</i>	
Male mutant	<i>MPK4/mpk4-2 ANQ/anq-2</i>				
Observed	27	38	23	20	
Expected	27	27	27	27	0.076>0.05
Female mutant	<i>MPK4/mpk4-2 ANQ/anq-2</i>				
Observed	85	79	29	9	
Expected	50.5	50.5	50.5	50.5	7.3E-18<0.05*
Viability		93%	34%	11%	

We determined the genotypes of 310 progeny from reciprocal crosses between *mpk4-2/+ anq-2/+* mutants and wild-type plants to infer the genotype of each gamete and the contribution by the mutant parent in each cross. The actual number of gametes observed for each genotype is shown. "Expected" indicates the number of gametes expected if all four possible gametes had been equally viable. Female viability was calculated from the observed number divided by 85. P values were calculated by the χ^2 test from observed and expected values. A P value indicative of a significant difference is indicated by an asterisk.

(Wassilewskija background) was outcrossed with the wild type (Col-0) three times or more. The progeny of these crosses were used for analyses.

The predicted amino acid sequence of MPK4 exhibits the strongest amino acid sequence similarity to that of MPK11 among members of the group B subfamily (88.3%; Figure 2E). A T-DNA insertion mutation in the *MPK11* gene resulted in plants with normal morphology, which were indistinguishable from wild-type plants (Figures 2G and 2H). The dwarfism of *mpk4-2 mpk11* double mutant plants was, however, more severe than that of the *mpk4-2* single mutant, and the petioles of the double mutant were much shorter than *mpk4-2* petioles (Figures 2I and 2J). The double mutant was unable to develop inflorescences. To quantify cytokinetic defects in *mpk11* and *mpk4-2 mpk11* plants, we counted the cells with incomplete cell walls in cotyledons of these mutants (Table 2). Although the cytokinetic defects in *mpk4-2* and *mpk4-2 mpk11* cotyledons were relatively weak compared with those in other organs, such as roots (Figure 1S; see Supplemental Figure 2 online), we chose to use cotyledons for quantitative analysis because of the small sizes of cells. We prepared series of transverse sections, starting from the middle, of the cotyledons of 9-d-old plants. There were no cell wall-defective cells in sections of *mpk11* cotyledons. However, the percentage of cells with incomplete cell walls in the *mpk4-2 mpk11* double mutant ($3.6\% \pm 0.76\%$ on average, $n = 6$) was significantly higher than in the *mpk4-2* single mutant ($1.9\% \pm 0.56\%$ on average, $n = 6$).

We also examined a T-DNA insertion mutant of the *MPK13* gene and the *mpk4-2 mpk13* double mutant for possible cytokinetic defects since the amino acid sequence of MPK13 also resembles that of tobacco NRK1/NTF6 more closely than do those of other MAPKs (Figure 2E). As shown in Supplemental Figure 3 online, there were no apparent abnormalities in the *mpk13* single mutant, and there was no significant phenotypic difference between the *mpk4-2* single mutant and the *mpk4-2 mpk13* double mutant. Supplemental Table 2 online shows that, on average, $2.5\% \pm 0.62\%$ ($n = 6$) and $2.1\% \pm 0.61\%$ ($n = 6$) of cells in the *mpk4-2* and *mpk4-2 mpk13* mutants had incomplete cell walls, respectively.

MPK4 Negatively Controls Expression of the *MPK11* Gene

We measured levels of *MPK11* transcripts in *mpk4-2* plants by quantitative real-time RT-PCR with poly(A)⁺ RNAs that had been prepared from shoot apices and cotyledons. In shoot apices, the level of *MPK11* transcripts was 40-fold higher in the *mpk4-2* mutant than in the wild type (Figure 3A). Levels of *MPK11* transcripts were also 12-fold higher in the mutant cotyledons (Figure 3B). Similar increases were also observed in *mpk4-1* leaves (see Supplemental Figure 4 online). However, levels of *MPK5*, *MPK12*, and *MPK13* transcripts in the shoot apices of *mpk4-2* were similar to those of in the shoot apices of wild-type plants. Levels of *MPK11* transcripts were very similar in the shoot apices of *mkk6-2/anq-2* and *nack1-3* mutants, which have defects in cytokinesis. Thus, marked increases in levels of *MPK11* transcripts appeared to be specific to plants with the mutation in the *MPK4* gene.

Molecular Relationships between MKK6/ANQ MAPKK and Group B MAPKs

We tested MAPKs for potential activation by MKK6/ANQ MAPKK using protoplasts of cells from *Arabidopsis* plants (Figure 4). Five cDNAs for hemagglutinin (HA)-tagged group B MAPKs (MPK4, MPK5, MPK11, MPK12, and MPK13) were coexpressed, separately, with cDNAs for kinase-inactive (L; amino acid substitution in the ATP binding site of subdomain II), wild-type (W), and constitutively active (G; amino acid substitutions by Asp residues) forms, respectively, of Myc-tagged MKK6/ANQ (MKK6/ANQ-Myc). After immunoprecipitation of each HA-tagged MAPK, we determined their activities in kinase assays in vitro with myelin basic protein (MBP) as an artificial substrate. MPK4, MPK5, and MPK13 were activated by the constitutively active MKK6/ANQ (Figure 4, G lanes). Activation of MPK13 by MKK6 was consistent with a previous observation by Melikant et al. (2004). MPK11 was only weakly activated. We also examined members of group C (MPK1, MPK2, MPK7, and MPK14), group A (MPK3 and MPK6), and group D (MPK8, MPK15, MPK16, MPK17, MPK18, and

Table 2. The Frequency of Cells with an Incomplete Cell Plate in Cotyledons

Genotype	No. of Cells with an Incomplete Cell Plate ^a	No. of Cells ^b	The Frequency of Cells with an Incomplete Cell Plate (%)
Col-0 #1	0	353	0
Col-0 #2	1	276	0.36
Col-0 #3	0	283	0
Col-0 #4	0	277	0
Col-0 #5	0	313	0
Col-0 #6	0	283	0
Average frequency			0.06 ± 0.15
<i>mpk11</i> #1	0	280	0
<i>mpk11</i> #2	0	323	0
<i>mpk11</i> #3	0	282	0
<i>mpk11</i> #4	0	334	0
<i>mpk11</i> #5	0	326	0
<i>mpk11</i> #6	0	320	0
Average frequency			0 ± 0
P value*			0.34>0.05
<i>mpk4-2</i> #1	4	207	1.9
<i>mpk4-2</i> #2	4	235	1.7
<i>mpk4-2</i> #3	5	248	2
<i>mpk4-2</i> #4	3	259	1.2
<i>mpk4-2</i> #5	7	243	2.9
<i>mpk4-2</i> #6	4	236	1.7
Average frequency			1.9 ± 0.56
P value*			1.50E-05<0.05
<i>mpk4-2 mpk11</i> #1	12	259	4.6
<i>mpk4-2 mpk11</i> #2	7	199	3.5
<i>mpk4-2 mpk11</i> #3	7	218	3.2
<i>mpk4-2 mpk11</i> #4	4	159	2.5
<i>mpk4-2 mpk11</i> #5	9	207	4.3
<i>mpk4-2 mpk11</i> #6	8	222	3.6
Average frequency			3.6 ± 0.76
P value*			5.20E-07<0.05
P value**			0.0012<0.05

^{a,b}Transverse sections (5 μm) were prepared from cotyledons of 9-d-old Col-0, *mpk11*, *mpk4-2*, and *mpk4-2 mpk11* seedlings. The number of cells and that of cells with incomplete cell plates was counted in a typical single section from cotyledons of six homozygous siblings (#1 to #6). Average frequencies are presented as means ± SD (*n* = 6). P values were calculated by Student's *t* test. A single asterisk indicates comparison with Col-0. Two asterisks indicate comparison with *mpk4-2*.

MPK19) for activation in similar assays. MPK1 activity was slightly increased by coexpression of constitutively active MKK6/ANQ-Myc, but other MAPKs that we tested were not activated (Figure 4; see Supplemental Figure 5 online).

MPK4 Is Active in the Presence of MKK6/ANQ in Tissues of *Arabidopsis* Plants That Contain Dividing Cells

We raised polyclonal MPK4-specific antibodies in rabbits, which were immunized with a synthetic oligopeptide that corresponded to amino acid residues 361 to 367 of MPK4. The antibodies recognized a single protein of 40 kD, which corresponds to the estimated molecular mass of MPK4, in a protein extract prepared from wild-type plants (see Supplemental Figure 6 online). The signal that corresponded to this protein was not detected in extracts prepared from the *mpk4-2* mutant, demonstrating that *mpk4-2* mutant plants failed to produce detectable amounts of MPK4.

We prepared protein extracts from wild-type and *mpk4-2* whole plants, developing first and second leaves, mature coty-

ledons, shoot apices, roots without tips, and root tips. Then, we performed immunocomplex kinase assays with the MPK4-specific antibodies and MBP as the artificial substrate. As shown in Figure 5A, we detected very weak activities of MPK4 protein kinase in protein extracts from whole wild-type and *mpk4-2* plants, respectively. The activity of MPK4 was clearly detected in extracts of developing leaves, shoot apices, and root tips (Figure 5A, lanes 3, 5, and 7), all of which contain actively dividing cells, but no clear activity was detected in extracts of mature cotyledons (lane 4) and roots without tips (lane 6) under the same conditions. These results suggested that MPK4 might be activated in tissues that contain dividing cells.

We examined whether a mutation in the *MKK6/ANQ* gene for a MAPKK that was involved in the activation of MPK4 (Figure 5B) might affect the activity of MPK4 in planta. We prepared protein extracts from developing first and second leaves plus shoot apices of wild-type plants, of *mpk4-2* mutant plants, and of *mkk6-2/anq-2* mutant plants and performed immunocomplex kinase assays with the MPK4-specific antibodies. Although

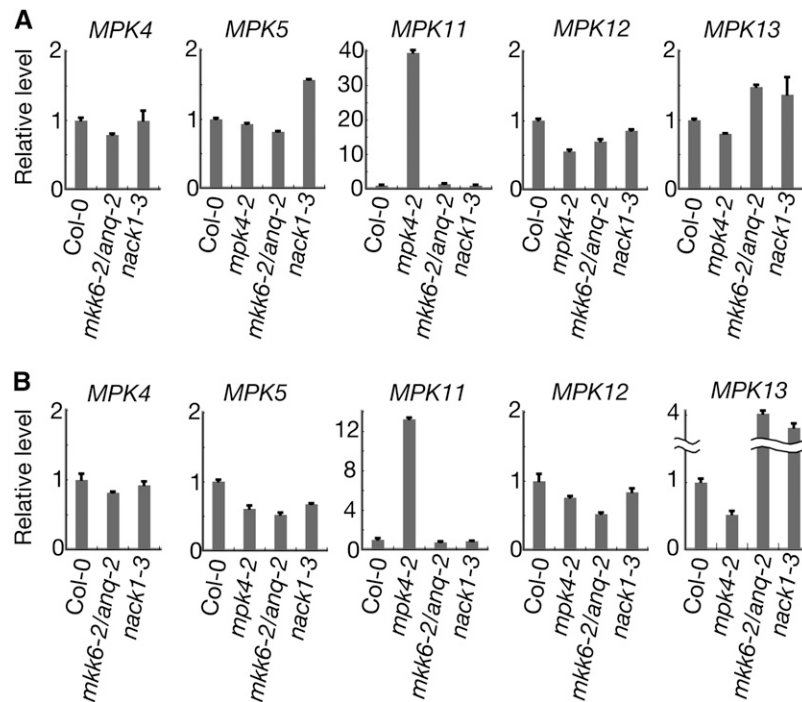


Figure 3. *MPK4* Represses the Accumulation of *MPK11* Transcripts.

(A) and **(B)** Quantitative RT-PCR was performed to determine the levels of transcripts of *MPK4*, *MPK5*, *MPK11*, *MPK12*, and *MPK13* in wild-type (Col-0), *mpk4-2*, *mkk6-2/anq-2*, and *nack1-3* plants. All plants analyzed here had the Col-0 background. Total RNA was prepared from the shoot apex **(A)** and cotyledons **(B)** of 9-d-old plants. After the reverse transcription reaction, the resultant cDNAs were amplified with primers specific for each respective gene. Quantitative RT-PCR data were normalized by reference to transcripts of the *EF1- α* gene. Values are shown relative to that for the wild type. Error bars indicate SD ($n = 3$).

kinase activity was clearly detected in the immunocomplex from the wild-type extract, lower levels of activity were detected in immunocomplexes from *mpk4-2* and *mkk6-2/anq-2* extracts (Figure 5B). These results were consistent with the observation that *MPK4* was activated in the presence of *MKK6/ANQ* in vivo (Figure 5B) and in vitro (Takahashi et al., 2010).

***MPK4* Is Localized to Cell Plates and Involved in Its Expansion in Cells in the Division Zone of Roots**

We generated transgenic *mpk4-2* plants that expressed a fusion of the entire *MPK4* locus with the cDNA construct for yellow fluorescent protein (YFP) at the C terminus (*MPK4-YFP*). In the transgenic plants, the *mpk4* dwarf phenotype was reversed, suggesting that *MPK4-YFP* was functional. Upon further examination of these plants, we observed signals due to YFP in the root cells in the division zone. Confocal microscopy revealed that signals due to *MPK4-YFP* in most of the cells were localized both in the cytoplasm and in the nucleus (Figures 6A and 6B), consistent with previous observations (Andreasson et al., 2005). In a significant proportion of the cells, however, signals due to YFP were concentrated in the region that corresponded to the cell division plane, both at early stages, when the nuclei had not yet reformed (indicated by arrows in Figures 6C and 6D), and later, when the two daughter nuclei had reformed (indicated by arrowheads in Figure 6E).

We stained root tips of the transgenic wild-type plant that expressed *MPK4-GFP* (for green fluorescent protein) with FM4-64 to label cell plates and observed signals due to GFP and FM4-64 in cells of the division zone. As shown in Figures 6F to 6H, *MPK4-GFP* was localized to the cell plate. Time-lapse analyses with FM4-64 demonstrated that the cell plate in wild-type root cells extended toward the parental cell walls in 15 min (Figure 6I), which is consistent with the recently reported observation (Fendrych et al., 2010). By contrast, cell plates in *mpk4-2* root cells slightly or barely expanded over 24 min (Figures 6J and 6K).

DISCUSSION

***MPK4* Is Involved in Cytokinesis in *Arabidopsis* Plants**

This study provides four lines of evidence for the involvement of *MPK4* in cytokinesis as follows: (1) *mpk4* mutant plants exhibited typical cytokinetic defects (Figure 1); (2) the defects were enhanced by the introduction of a mutation in the *MKK6/ANQ* gene for MAPKK, which is involved in cytokinesis (Soyano et al., 2003), into the *mpk4* mutant (Figure 2, Table 1; see Supplemental Table 1 online); (3) *MPK4* activity was detected only in organs that contain dividing cells in *Arabidopsis* plants (Figure 5A), and *MPK4* activity was detected in the presence *MKK6/ANQ* MAPKK (Figures 4 and 5B); and (4) the fluorescent protein-fused *MPK4*

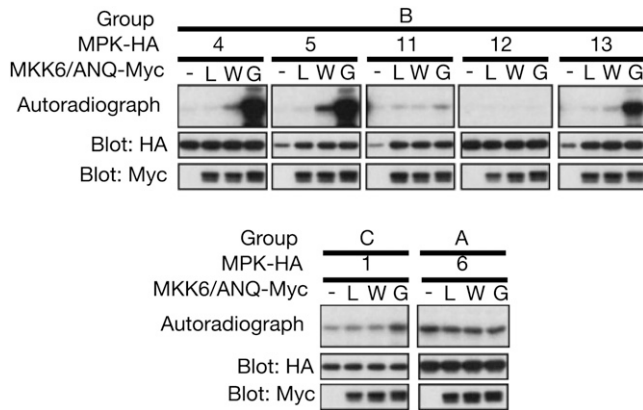


Figure 4. Identification of Candidate MAPKs (MPK4, MPK5, MPK11, MPK12, and MPK13) Downstream of MKK6/ANQ MAPKK.

DNA constructs for the various HA-tagged MAPKs (MAPK-HA) were transiently introduced into protoplasts of *Arabidopsis*. Activation of MAPKs was examined by coexpression of Myc-tagged MKK6/ANQ (MKK6/ANQ-Myc) with a kinase-inactive domain (L), the wild-type domain (W), or a constitutively active domain (G). The kinase activity of MAPK-HA that had been immunoprecipitated with HA-specific antibodies was assayed with MBP as substrate, and [γ - 32 P]ATP phosphorylation of MBP was quantitated by autoradiography after SDS-PAGE. MAPK-HA and MKK6/ANQ-Myc proteins were detected by protein gel blotting with HA-specific (for MAPKs) and Myc-specific (for MKK6/ANQ) antibodies, respectively.

proteins were localized to the cell plate in cells in root tips (Figures 6A to 6H). Expansion of the cell plate was aberrant in dividing cells of the *mpk4-2* mutant (Figures 6I to 6K).

We also performed aniline blue staining to observe newly synthesized cell plates in cells of the root division zone (see Supplemental Figure 7 online). Most cells in the wild-type plant contained complete cell plates. Although some cells in *mpk4-2* also had complete cell plates (arrowheads), many cells, which were nearly normal in size, showed incomplete cell plates (arrows). In addition, the abnormal direction of the formation of the cell plates, most of which showed irregular thickness, was observed in *mpk4-2*, showing that MPK4 affects the direction of the cell plate formation and patterns of callose accumulation. These results suggest that MPK4 is involved not only in the simple expansion of the cell plates but also in various aspects of cytokinesis. However, to understand how MPK4 can control these events, further biochemical and cell biological studies of MPK4 and its targets are required.

We demonstrated that the NRK1 MAPK of tobacco cells phosphorylates MAP65-1 and that phosphorylation of MAP65-1 reduces its MT-bundling activity, thereby enhancing the destabilization and turnover of MTs and perhaps the expansion of phragmoplast (Sasabe et al., 2006). Recently, we also showed that GFP-MAP65-3 and MPK4-GFP are concentrated at the division plane in the phragmoplast (see Supplemental Figure 8 online) and that MPK4 phosphorylates the MAP65-3/PLE protein (see Supplemental Figure 9 online), which plays an essential role in cytokinesis (Müller et al., 2004), suggesting that MPK4 plays a role in the turnover of MTs during cytokinesis.

It has been reported that MPK4 also plays a role in the defense response that is induced by plant pathogens and salicylic acid. It has been proposed that MPK4 is a negative regulator of the pathogen response since this response is induced constitutively in the *mpk4-1* mutant (Petersen et al., 2000). We failed to find any defects in formation of the cell plate in the *mpk4-1* mutant with the *Ler* background, even though such plants exhibited a dwarf phenotype, consistent with previously published observations (Petersen et al., 2000). However, this study showed that when the *mpk4-1* allele was transferred to the Col-0 background, plants exhibited typical defects in formation of the cell plate, resembling *mpk4-2* plants with this background. These results suggest that the abnormality related to cytokinesis was suppressed on the genetic background (*Ler*) of the original *mpk4-1* isolate. In addition, we detected the transcript from which the intron with the transposon sequence had been excised normally in *mpk4-1* plants, even though the level of the MPK4 transcript was lower than in the wild type (Figure 1F). This result also suggests that *mpk4-1* is a weak allele.

Although *mpk4-2* is a transcription-null allele, formation of the cell plate in the corresponding mutant plants was not completely defective. The phenotype was clearly distinct from the lethal phenotype observed in the case of gametophytes of the *anp1 anp2 anp3* triple mutant (Krysan et al., 2002) and the *hinkel/nack1*

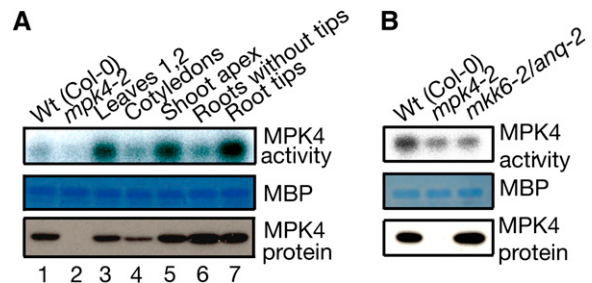


Figure 5. Elevated Activity of MPK4 Protein Kinase in Organs and Tissues That Contain Dividing Cells.

(A) Endogenous activities of MPK4 in various organs. Protein extracts were obtained from the indicated organs and tissues of Col-0 wild-type (Wt) and *mpk4-2* 9-d-old plants. Immunocomplex kinase assays were performed with MPK4-specific antibodies and MBP as substrate. Whole wild-type (1) and *mpk4-2* (2) plants, and the developing first and second leaves (3), cotyledons (4), shoot apices (5), roots without tips (6), and root tips (7) of wild-type plants were examined (top). MBP was visualized after staining with Coomassie blue (middle). Endogenous levels of MPK4 protein in the various organs are shown in the bottom panel. Extracts used for immunocomplex kinase assays were immunoblotted with MPK4-specific antibodies. Twenty micrograms of protein were loaded in each lane.

(B) Endogenous activity of MPK4 protein kinase in the wild-type (Col-0), *mpk4-2*, and *mkk6-2/anq-2* plants. Immunocomplex kinase assays were performed with MPK4-specific antibodies as described above (top). The protein extracts were obtained from developing first and second leaves plus shoot apices of wild-type, *mpk4-2*, and *mkk6-2/anq-2* plants. MBP was visualized after staining with Coomassie blue (middle). Levels of MPK4 proteins are shown in the bottom panel. Extracts used for immunocomplex kinase assays were immunoblotted with MPK4-specific antibodies. Twenty micrograms of protein were loaded in each lane. The signal detected in the case of *mpk4-2* was due to nonspecific MAPK.

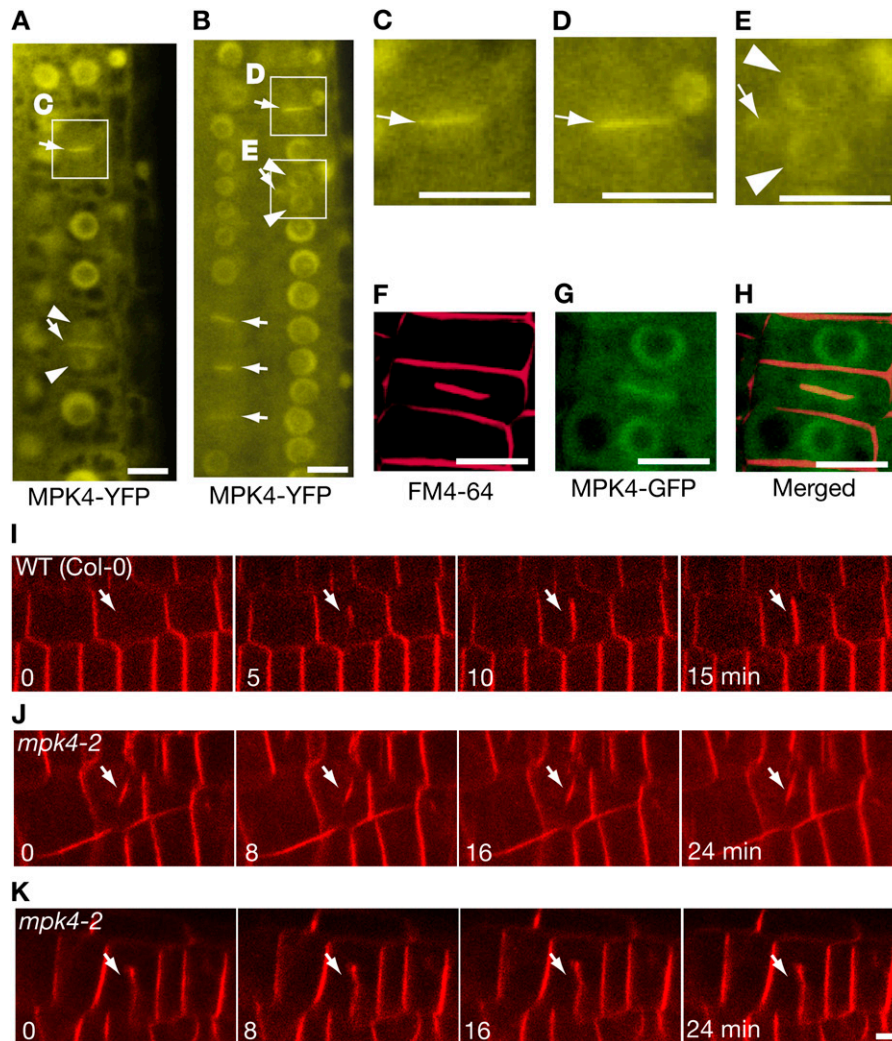


Figure 6. MPK4 Is Localized to Cell Plates and Involved in Its Expansion in Cells in the Division Zone of Roots.

(A) and (B) The photographs, taken under a confocal microscope, show the fluorescence due to YFP in the root tip of a transgenic plant that expressed the fusion gene composed of the entire *MPK4* locus and YFP cDNA.

(C) to (E) Magnified views of boxed regions that are shown in (A) and (B). Arrows and arrowheads indicate regions that appeared to correspond to the division plane of the cells and the two newly formed nuclei, respectively.

(F) to (H) Fluorescence micrographs show the fluorescence due to FM4-64 (F) and MPK4-GFP (G) in the root tip of a transgenic plant that expressed the fusion gene composed of the entire *MPK4* locus and GFP cDNA. Merged images are shown in (H). Bars = 10 μ m.

(I) to (K) Time series of growing cell plates stained with FM4-64 in root tips of 3-d-old wild-type (I) and *mpk4-2* (J) and (K) plants. Arrows indicate the growing or arrested cell plates. Cells in these pictures are located 70 to 90 μ m above quiescent center. Bars = 5 μ m.

stud/tet/nack2 double mutant (Tanaka et al., 2004). Our observations suggest the presence of at least one other factor that function redundantly in cytokinesis, as discussed below.

MPK4 Functions in a Variety of Physiological Processes, Depending on the Tissue and Organ in Which It Is Expressed

In addition to its participation in the defense responses, as mentioned in the previous section, the activity of MPK4 responds to various external stimuli, such as infection by pathogens and treatment with the bacterial elicitor flagellin (Mészáros et al.,

2006), cold stress, and salt stress (Teige et al., 2004). In the response to flagellin, the MAPKK MKK1 is involved in the activation of MPK4, while MAPKK MKK2 is a direct activator of MPK4 in the response to cold stress and salt stress. Ichimura et al. (2006) reported that activation of MPK4 requires the MAPKKK MEKK1, which negatively regulates a specific type of cell death. Furthermore, Beck et al. (2010) reported recently that MPK4 is essential for the proper organization of cortical MTs in epidermal cells via the phosphorylation of MAP65-1. Since the MPK4 protein is present in many organs, including mature as well as developing leaves (Figure 5A), it is possible that it participates

time with a real-time PCR system (model 7500; Applied Biosystems). The results were normalized by reference to results for *EF1- α* or *β -tubulin*. Details of the method were described by Matsumura et al. (2009). Primers used for the experiments are listed in Supplemental Table 3 online.

Histological Analysis

Plant materials were prepared for sectioning as described by Semiarti et al. (2001) and Iwakawa et al. (2007).

Transient Protein Expression Assays

The open reading frames of genes for MPKs and MKK6/ANQ were cloned into the plant expression vector pRT100 (Töpfer et al., 1987; Kiegerl et al., 2000) such that gene products were fused at their C-terminal ends either to a triple HA epitope (MPKs) or to a double c-myc epitope (MKK6/ANQ). Primers used for cloning are listed in Supplemental Table 3 online. Transient protein expression assays in *Arabidopsis* protoplasts were performed as described previously (Ouaked et al., 2003).

Preparation of Protein Extracts from *Arabidopsis* Protoplasts and Plants

Protein extracts were prepared either from protoplasts as described previously (Cardinale et al., 2002) or from frozen *Arabidopsis* plants in TG150 buffer (25 mM Tris-HCl, pH 7.5, 10 mM EDTA, 10 mM EGTA, 150 mM NaCl, 10% glycerol, 0.01% Triton X-100, 1 mM DTT, 20 mM β -glycerophosphate, 1 mM sodium-*o*-vanadate, 1 mM phenylmethane-sulfonyl fluoride, and 5 μ g/mL each of leupeptin, chymostatin, pepstatin A, and antipain). Proteins in extracts from protoplasts and plants were quantified with a protein assay kit (Bio-Rad) with BSA as the standard.

Production of Antibodies and Immunodetection of Proteins

Antibodies against MPK4 were prepared by immunizing rabbits with the synthetic peptide ELIYRETVKFNPQDSV (residues 361 to 376 of MPK4), which was synthesized by MBL. Antibodies were affinity purified with the immobilized antigen, which was prepared using the SulfoLink immobilization kit for peptides (Thermo Scientific). SDS-PAGE and immunoblotting were performed as described previously by Nishihama et al. (2001). For detection of MPK4, we used specific affinity-purified antibodies at a concentration of 0.5 μ g/mL. For detection of HA- and Myc-fusion proteins, we used HA-specific (clone 12CA5) and Myc-specific (clone 9E10) monoclonal antibodies, as described previously (Nakagami et al., 2004).

Immunocomplex Kinase Assays

Immunocomplex kinase assays, using proteins extracted from protoplasts, were performed as described by Nakagami et al. (2004). Immunocomplex kinase assays using proteins extracted from plants were performed as described by Nishihama et al. (2001). In brief, protein extracts (250 μ g of protein) were diluted to 200 μ L with TG150 buffer (see above) and incubated with 1 μ g of MPK4-specific antibodies at 25°C for 2 h. Then, they were incubated with 20 μ L of a 50% slurry of rProtein A-Sepharose 4 Fast Flow (GE Healthcare) at 4°C for 1 h. The resin was washed three times with TG150 buffer and twice with kinase buffer, which contained 50 mM HEPES-KOH, pH 7.5, 20 mM MgCl₂, 5 mM EGTA, 1 mM DTT, 20 mM β -glycerophosphate, and 1 mM sodium-*o*-vanadate. The resin was resuspended in a reaction cocktail (20 μ L) that included 5 μ g of MBP, 50 μ M ATP, and 10 μ Ci of [γ -³²P]ATP (GE Healthcare) in kinase buffer and incubated at 25°C for 30 min. After addition of 20 μ L of 2 \times SDS sample buffer and boiling, samples were subjected to SDS-PAGE and radioactivity was visualized with an imaging analyzer (BAS-1800; Fujifilm).

Construction of the *MPK4-YFP* and *MPK4-GFP* Fusion Genes

The *MPK4* locus upstream (2693 bp) and downstream (258 bp) of the termination codon was amplified from Col-0 genomic DNA with specific primers (see Supplemental Table 3 online). The open reading frame for YFP was amplified with the primer set YFP_F/YFP_R from pEXCS-GW-mYFP-nls (kindly provided by Jane Parker; see Supplemental Table 3 online). All PCR fragments were generated using iProof (Bio-Rad), ligated by T/A cloning in pGEMTeasy (Promega), and sequenced. Using appropriate restriction enzymes (see Supplemental Table 3 online), we reassembled the *MPK4* locus in pGREEN0229 to generate pGREEN0229-MPK4L. Next, the *Bam*HI-*Bgl*II DNA fragment encoding YFP was cloned at the unique compatible *Bam*HI locus to generate pGREEN0229-MPK4L-YFP. The *MPK4* locus that covered from the region upstream (2966 bp) of the termination codon to the codon before the termination codon was amplified from Col-0 genomic DNA with the primer set KK93/KK138 (see Supplemental Table 3 online). The PCR fragments were cloned into the pGWB4 vector (Nakagawa et al., 2007). Wild-type plants (Col-0) were transformed with *Agrobacterium tumefaciens* by the floral dip method (Clough and Bent, 1998). Basta-resistant plants were genotyped for the *MPK4* locus with the primer sets K4WT_S/K4WT_R for amplification of the wild-type allele-specific fragment and LB6316/K4WT_R for amplification of the *mpk4-2* allele-specific fragment, respectively.

Microscopy

Signals due to YFP were monitored with a confocal microscope (TCS SP2-AOBS; Leica). Plants were grown on Murashige and Skoog (MS) medium (half-strength MS, 1% sucrose, and 0.5% MES, pH 5.4; Agar Type E) for 4 d. Signals due to GFP and FM4-64 were monitored with a confocal microscope (LSM510; Carl Zeiss). FM4-64 (Invitrogen) was solubilized in DMSO to a concentration of 2 mM and diluted 1:200 in water, and the diluted solution was added to roots of 5-d-old plants placed on a Gellan gum plate and incubated for 10 min prior to observation. Live-cell imaging was performed using 3- to 4-d-old seedlings. The seedlings were stained with 6.4 mM FM4-64 (Invitrogen) in MS buffer for 10 min and put onto the chambered cover slides (Lab-Tek II; Thermo Scientific). The chambered cover slides were placed on the inverted platform of a fluorescence microscope (IX-81; Olympus) equipped with a CSUX-1 confocal laser scanner unit (Yokogawa Electronic) and a CCD camera (CoolSNAP HQ2; Roper Scientific). Images were acquired with a \times 40 objective lens (UPLFLN40, numerical aperture 1.3, oil immersion) using diode-pumped solid-state 561-nm lasers (Melles Griot). The time-lapse images were processed with Metamorph version 7.5 (Molecular Devices).

Accession Numbers

Sequence data from this article can be found in the Arabidopsis Genome Initiative under the following accession numbers: *MPK4* (At4g01370), *MPK5* (At4g11330), *MPK11* (At1g01560), *MPK12* (At2g46070), *MPK13* (At1g07880), *ANQ/MKK6* (At5g56580), *MAP65-3/PLE* (At5g51600), *EF1- α* (At5g60390), and *β -tubulin* (At5g12250).

Supplemental Data

The following materials are available in the online version of this article.

Supplemental Figure 1. Complementation of the *mpk4-2* Mutation by the 3.6-kb Fragment of Genomic DNA That Encompassed the *MPK4* Locus.

Supplemental Figure 2. Cytokinetic Defects in Roots of *mpk4-2* and *mpk-2 mpk11* Mutant Plants.

Supplemental Figure 3. Comparison of the Phenotypes of the *mpk4-2 mpk13* Double Mutant with That of each Respective Single Mutant.

Supplemental Figure 4. Accumulation of Transcripts of the *MPK11* Gene in *mpk4-1* and *mpk4-2* Mutants.

Supplemental Figure 5. Activation of Various MPKs in Protoplasts by MKK6/ANQ.

Supplemental Figure 6. Specificity of MPK4-Specific Antibodies.

Supplemental Figure 7. Confocal Sections of Wild-Type and *mpk4-2* Root Tips Stained with Aniline Blue.

Supplemental Figure 8. Subcellular Localization of MPK4-GFP and GFP-MAP65-3/PLE in Tobacco BY-2 Cells at Telophase.

Supplemental Figure 9. Phosphorylation of MAP65-3/PLE In Vitro by Active MPK4.

Supplemental Table 1. The Progeny of Crosses between *MPK4/mpk4-2* and *ANQ/anq-2*.

Supplemental Table 2. The Frequency of Cells with an Incomplete Cell Wall.

Supplemental Table 3. Primers Used in This Study.

Supplemental Data Set 1. Text File of the Alignment Used for the Phylogenetic Analysis Shown in Figure 2F.

ACKNOWLEDGMENTS

This work was supported in part by a grant from the Program for the Promotion of Basic Research Activities for Innovative Biosciences, by a Grant-in-Aid for Scientific Research on Priority Areas (19060003), and by a Grant-in-Aid for the 21st Century Center of Excellence (COE) Program (Systems Bioscience) awarded to the Division of Biological Science of Nagoya University from the Ministry of Education, Culture, Sports, Science and Technology of Japan. K.K. was supported by a Grant-in-Aid for the Global COE program, awarded to the Division of Biological Science of Nagoya University.

Received June 6, 2010; revised October 9, 2010; accepted October 29, 2010; published November 23, 2010.

REFERENCES

- Alonso, J.M., et al. (2003). Genome-wide insertional mutagenesis of *Arabidopsis thaliana*. *Science* **301**: 653–657.
- Andreasson, E., et al. (2005). The MAP kinase substrate MKS1 is a regulator of plant defense responses. *EMBO J.* **24**: 2579–2589.
- Asada, T., Sonobe, S., and Shibaoka, H. (1991). Microtubule translocation in the cytokinesis apparatus of cultured tobacco cells. *Nature* **350**: 238–241.
- Banno, H., Hirano, K., Nakamura, T., Irie, K., Nomoto, S., Matsumoto, K., and Machida, Y. (1993). *NPK1*, a tobacco gene that encodes a protein with a domain homologous to yeast BCK1, STE11, and Byr2 protein kinases. *Mol. Cell. Biol.* **13**: 4745–4752.
- Beck, M., Komis, G., Müller, J., Menzel, D., and Samaj, J. (2010). *Arabidopsis* homologs of nucleus- and phragmoplast-localized kinase 2 and 3 and mitogen-activated protein kinase 4 are essential for microtubule organization. *Plant Cell* **22**: 755–771.
- Bögge, L., Calderini, O., Binarova, P., Mattauch, M., Till, S., Kiegerl, S., Jonak, C., Pollaschek, C., Barker, P., Huskisson, N.S., Hirt, H., and Heberle-Bors, E. (1999). A MAP kinase is activated late in plant mitosis and becomes localized to the plane of cell division. *Plant Cell* **11**: 101–113.
- Calderini, O., Bögge, L., Vicente, O., Binarova, P., Heberle-Bors, E., and Wilson, C. (1998). A cell cycle regulated MAP kinase with a possible role in cytokinesis in tobacco cells. *J. Cell Sci.* **111**: 3091–3100.
- Cardinale, F., Meskiene, I., Ouaked, F., and Hirt, H. (2002). Convergence and divergence of stress-induced mitogen-activated protein kinase signaling pathways at the level of two distinct mitogen-activated protein kinase kinases. *Plant Cell* **14**: 703–711.
- Clough, S.J., and Bent, A.F. (1998). Floral dip: A simplified method for *Agrobacterium*-mediated transformation of *Arabidopsis thaliana*. *Plant J.* **16**: 735–743.
- Fendrych, M., Synek, L., Pecenkova, T., Toupalova, H., Cole, R., Drdova, E., Nebesárova, J., Sedínová, M., Hála, M., Fowler, J.E., and Zársky, V. (2010). The *Arabidopsis* exocyst complex is involved in cytokinesis and cell plate maturation. *Plant Cell* **22**: 3053–3065.
- Gu, X., and Verma, D.P. (1996). Phragmoplastin, a dynamin-like protein associated with cell plate formation in plants. *EMBO J.* **15**: 695–704.
- Hamada, S., Onouchi, H., Tanaka, H., Kudo, M., Liu, Y.G., Shibata, D., Machida, C., and Machida, Y. (2000). Mutations in the *WUSCHEL* gene of *Arabidopsis thaliana* result in the development of shoots without juvenile leaves. *Plant J.* **24**: 91–101.
- Hush, J.M., Wadsworth, P., Callaham, D.A., and Hepler, P.K. (1994). Quantification of microtubule dynamics in living plant cells using fluorescence redistribution after photobleaching. *J. Cell Sci.* **107**: 775–784.
- Ichimura, K., Casais, C., Peck, S.C., Shinozaki, K., and Shirasu, K. (2006). MEKK1 is required for MPK4 activation and regulates tissue-specific and temperature-dependent cell death in *Arabidopsis*. *J. Biol. Chem.* **281**: 36969–36976.
- Ichimura, K., et al; MAPK Group (2002). Mitogen-activated protein kinase cascades in plants: A new nomenclature. *Trends Plant Sci.* **7**: 301–308.
- Ishikawa, M., Soyano, T., Nishihama, R., and Machida, Y. (2002). The NPK1 mitogen-activated protein kinase kinase kinase contains a functional nuclear localization signal at the binding site for the NACK1 kinesin-like protein. *Plant J.* **32**: 789–798.
- Iwakawa, H., Iwasaki, M., Kojima, S., Ueno, Y., Soma, T., Tanaka, H., Semiarti, E., Machida, Y., and Machida, C. (2007). Expression of the *ASYMMETRIC LEAVES2* gene in the adaxial domain of *Arabidopsis* leaves represses cell proliferation in this domain and is critical for the development of properly expanded leaves. *Plant J.* **51**: 173–184.
- Jürgens, G. (2005). Plant cytokinesis: Fission by fusion. *Trends Cell Biol.* **15**: 277–283.
- Kasahara, K., Nakayama, Y., Nakazato, Y., Ikeda, K., Kuga, T., and Yamaguchi, N. (2007). Src signaling regulates completion of abscission in cytokinesis through ERK/MAPK activation at the midbody. *J. Biol. Chem.* **282**: 5327–5339.
- Kawabe, A., Matsunaga, S., Nakagawa, K., Kurihara, D., Yoneda, A., Hasezawa, S., Uchiyama, S., and Fukui, K. (2005). Characterization of plant Aurora kinases during mitosis. *Plant Mol. Biol.* **58**: 1–13.
- Kiegerl, S., Cardinale, F., Siligan, C., Gross, A., Baudouin, E., Liwosz, A., Eklöf, S., Till, S., Bögge, L., Hirt, H., and Meskiene, I. (2000). SIMKK, a mitogen-activated protein kinase (MAPK) kinase, is a specific activator of the salt stress-induced MAPK, SIMK. *Plant Cell* **12**: 2247–2258.
- Krysan, P.J., Jester, P.J., Gottwald, J.R., and Sussman, M.R. (2002). An *Arabidopsis* mitogen-activated protein kinase kinase kinase gene family encodes essential positive regulators of cytokinesis. *Plant Cell* **14**: 1109–1120.
- Krysan, P.J., Young, J.C., and Sussman, M.R. (1999). T-DNA as an insertional mutagen in *Arabidopsis*. *Plant Cell* **11**: 2283–2290.
- Matsumura, Y., Iwakawa, H., Machida, Y., and Machida, C. (2009). Characterization of genes in the *ASYMMETRIC LEAVES2/LATERAL ORGAN BOUNDARIES (AS2/LOB)* family in *Arabidopsis thaliana*, and

- functional and molecular comparisons between AS2 and other family members. *Plant J.* **58**: 525–537.
- Mayer, U., and Jürgens, G.** (2004). Cytokinesis: Lines of division taking shape. *Curr. Opin. Plant Biol.* **7**: 599–604.
- Melikant, B., Giuliani, C., Halbmayer-Watzina, S., Limmongkon, A., Heberle-Bors, E., and Wilson, C.** (2004). The *Arabidopsis thaliana* MEK AtMKK6 activates the MAP kinase AtMPK13. *FEBS Lett.* **576**: 5–8.
- Mészáros, T., Helfer, A., Hatzimasoura, E., Magyar, Z., Serazetdinova, L., Rios, G., Bardóczy, V., Teige, M., Koncz, C., Peck, S., and Bögre, L.** (2006). The *Arabidopsis* MAP kinase kinase MKK1 participates in defence responses to the bacterial elicitor flagellin. *Plant J.* **48**: 485–498.
- Müller, J., Beck, M., Metzbach, U., Komis, G., Hause, G., Menzel, D., and Samaj, J.** (2010). *Arabidopsis* MPK6 is involved in cell division plane control during early root development, and localizes to the pre-prophase band, phragmoplast, trans-Golgi network and plasma membrane. *Plant J.* **61**: 234–248.
- Müller, S., Smertenko, A., Wagner, V., Heinrich, M., Hussey, P.J., and Hauser, M.T.** (2004). The plant microtubule-associated protein AtMAP65-3/PLE is essential for cytokinetic phragmoplast function. *Curr. Biol.* **14**: 412–417.
- Nakagami, H., Kiegerl, S., and Hirt, H.** (2004). OMTK1, a novel MAPKKK, channels oxidative stress signaling through direct MAPK interaction. *J. Biol. Chem.* **279**: 26959–26966.
- Nakagawa, T., Kurose, T., Hino, T., Tanaka, K., Kawamukai, M., Niwa, Y., Toyooka, K., Matsuoka, K., Jinbo, T., and Kimura, T.** (2007). Development of series of gateway binary vectors, pGWBs, for realizing efficient construction of fusion genes for plant transformation. *J. Biosci. Bioeng.* **104**: 34–41.
- Nishihama, R., Banno, H., Kawahara, E., Irie, K., and Machida, Y.** (1997). Possible involvement of differential splicing in regulation of the activity of *Arabidopsis* ANP1 that is related to mitogen-activated protein kinase kinase kinases (MAPKKKs). *Plant J.* **12**: 39–48.
- Nishihama, R., Ishikawa, M., Araki, S., Soyano, T., Asada, T., and Machida, Y.** (2001). The NPK1 mitogen-activated protein kinase kinase is a regulator of cell-plate formation in plant cytokinesis. *Genes Dev.* **15**: 352–363.
- Nishihama, R., and Machida, Y.** (2001). Expansion of the phragmoplast during plant cytokinesis: A MAPK pathway may MAP it out. *Curr. Opin. Plant Biol.* **4**: 507–512.
- Nishihama, R., Soyano, T., Ishikawa, M., Araki, S., Tanaka, H., Asada, T., Irie, K., Ito, M., Terada, M., Banno, H., Yamazaki, Y., and Machida, Y.** (2002). Expansion of the cell plate in plant cytokinesis requires a kinesin-like protein/MAPKKK complex. *Cell* **109**: 87–99.
- Ouaked, F., Rozhon, W., Lecourieux, D., and Hirt, H.** (2003). A MAPK pathway mediates ethylene signaling in plants. *EMBO J.* **22**: 1282–1288.
- Petersen, M., et al.** (2000). *Arabidopsis* map kinase 4 negatively regulates systemic acquired resistance. *Cell* **103**: 1111–1120.
- Pollard, T.D.** (2010). Mechanics of cytokinesis in eukaryotes. *Curr. Opin. Cell Biol.* **22**: 50–56.
- Reichardt, I., Stierhof, Y.D., Mayer, U., Richter, S., Schwarz, H., Schumacher, K., and Jürgens, G.** (2007). Plant cytokinesis requires *de novo* secretory trafficking but not endocytosis. *Curr. Biol.* **17**: 2047–2053.
- Samuels, A.L., Giddings, T.H., Jr., and Staehelin, L.A.** (1995). Cytokinesis in tobacco BY-2 and root tip cells: A new model of cell plate formation in higher plants. *J. Cell Biol.* **130**: 1345–1357.
- Sasabe, M., and Machida, Y.** (2006). MAP65: A bridge linking a MAP kinase to microtubule turnover. *Curr. Opin. Plant Biol.* **9**: 563–570.
- Sasabe, M., Soyano, T., Takahashi, Y., Sonobe, S., Igarashi, H., Itoh, T.J., Hidaka, M., and Machida, Y.** (2006). Phosphorylation of NtMAP65-1 by a MAP kinase down-regulates its activity of microtubule bundling and stimulates progression of cytokinesis of tobacco cells. *Genes Dev.* **20**: 1004–1014.
- Semiarti, E., Ueno, Y., Tsukaya, H., Iwakawa, H., Machida, C., and Machida, Y.** (2001). The *ASYMMETRIC LEAVES2* gene of *Arabidopsis thaliana* regulates formation of a symmetric lamina, establishment of venation and repression of meristem-related homeobox genes in leaves. *Development* **128**: 1771–1783.
- Shapiro, P.S., Vaisberg, E., Hunt, A.J., Tolwinski, N.S., Whalen, A.M., McIntosh, J.R., and Ahn, N.G.** (1998). Activation of the MKK/ERK pathway during somatic cell mitosis: direct interactions of active ERK with kinetochores and regulation of the mitotic 3F3/2 phosphoantigen. *J. Cell Biol.* **142**: 1533–1545.
- Soyano, T., Nishihama, R., Morikiyo, K., Ishikawa, M., and Machida, Y.** (2003). NQK1/NtMEK1 is a MAPKK that acts in the NPK1 MAPKKK-mediated MAPK cascade and is required for plant cytokinesis. *Genes Dev.* **17**: 1055–1067.
- Strompen, G., El Kasmi, F., Richter, S., Lukowitz, W., Assaad, F.F., Jürgens, G., and Mayer, U.** (2002). The *Arabidopsis* HINKEL gene encodes a kinesin-related protein involved in cytokinesis and is expressed in a cell cycle-dependent manner. *Curr. Biol.* **12**: 153–158.
- Takahashi, Y., Soyano, T., Kosetsu, K., Sasabe, M., and Machida, Y.** (2010). HINKEL kinesin, ANP MAPKKKs and MKK6/ANQ MAPKK, which phosphorylates and activates MPK4 MAPK, constitute a pathway that is required for cytokinesis in *Arabidopsis thaliana*. *Plant Cell Physiol.* **51**: 1766–1776.
- Tanaka, H., Ishikawa, M., Kitamura, S., Takahashi, Y., Soyano, T., Machida, C., and Machida, Y.** (2004). The *AtNACK1/HINKEL* and *STUD/TETRASPORE/AtNACK2* genes, which encode functionally redundant kinesins, are essential for cytokinesis in *Arabidopsis*. *Genes Cells* **9**: 1199–1211.
- Tanaka, H., Onouchi, H., Kondo, M., Hara-Nishimura, I., Nishimura, M., Machida, C., and Machida, Y.** (2001). A subtilisin-like serine protease is required for epidermal surface formation in *Arabidopsis* embryos and juvenile plants. *Development* **128**: 4681–4689.
- Teige, M., Scheikl, E., Eulgem, T., Dóczi, R., Ichimura, K., Shinozaki, K., Dangl, J.L., and Hirt, H.** (2004). The MKK2 pathway mediates cold and salt stress signaling in *Arabidopsis*. *Mol. Cell* **15**: 141–152.
- Töpfer, R., Matzeit, V., Gronenborn, B., Schell, J., and Steinbiss, H.H.** (1987). A set of plant expression vectors for transcriptional and translational fusions. *Nucleic Acids Res.* **15**: 5890.
- Verma, D.P.S.** (2001). Cytokinesis and building of the cell plate in plants. *Annu. Rev. Plant Physiol. Plant Mol. Biol.* **52**: 751–784.
- Woollard, A.A., and Moore, I.** (2008). The functions of Rab GTPases in plant membrane traffic. *Curr. Opin. Plant Biol.* **11**: 610–619.
- Xing, Y., Jia, W., and Zhang, J.** (2008). AtMKK1 mediates ABA-induced *CAT1* expression and H₂O₂ production via AtMPK6-coupled signaling in *Arabidopsis*. *Plant J.* **54**: 440–451.
- Yang, C.Y., Spielman, M., Coles, J.P., Li, Y., Ghelani, S., Bourdon, V., Brown, R.C., Lemmon, B.E., Scott, R.J., and Dickinson, H.G.** (2003). *TETRASPORE* encodes a kinesin required for male meiotic cytokinesis in *Arabidopsis*. *Plant J.* **34**: 229–240.
- Yasuhara, H., and Shibaoka, H.** (2000). Inhibition of cell-plate formation by brefeldin A inhibited the depolymerization of microtubules in the central region of the phragmoplast. *Plant Cell Physiol.* **41**: 300–310.
- Yasuhara, H., Sonobe, S., and Shibaoka, H.** (1995). Effects of brefeldin A on the formation of the cell plate in tobacco BY-2 cells. *Eur. J. Cell Biol.* **66**: 274–281.
- Zecevic, M., Catling, A.D., Eblen, S.T., Renzi, L., Hittle, J.C., Yen, T.J., Gorbsky, G.J., and Weber, M.J.** (1998). Active MAP kinase in mitosis: Localization at kinetochores and association with the motor protein CENP-E. *J. Cell Biol.* **142**: 1547–1558.
- Zuo, J., Niu, Q.W., Nishizawa, N., Wu, Y., Kost, B., and Chua, N.H.** (2000). KORRIGAN, an *Arabidopsis* endo-1,4- β -glucanase, localizes to the cell plate by polarized targeting and is essential for cytokinesis. *Plant Cell* **12**: 1137–1152.

The MAP Kinase MPK4 Is Required for Cytokinesis in *Arabidopsis thaliana*

Ken Kosetsu, Sachihito Matsunaga, Hirofumi Nakagami, Jean Colcombet, Michiko Sasabe, Takashi Soyano, Yuji Takahashi, Heribert Hirt and Yasunori Machida
PLANT CELL published online Nov 23, 2010;
DOI: 10.1105/tpc.110.077164

This information is current as of November 25, 2010

Supplemental Data	http://www.plantcell.org/cgi/content/full/tpc.110.077164/DC1
Permissions	https://www.copyright.com/ccc/openurl.do?sid=pd_hw1532298X&iissn=1532298X&WT.mc_id=pd_hw1532298X
eTOCs	Sign up for eTOCs for <i>THE PLANT CELL</i> at: http://www.plantcell.org/subscriptions/etoc.shtml
CiteTrack Alerts	Sign up for CiteTrack Alerts for <i>Plant Cell</i> at: http://www.plantcell.org/cgi/alerts/ctmain
Subscription Information	Subscription information for <i>The Plant Cell</i> and <i>Plant Physiology</i> is available at: http://www.aspb.org/publications/subscriptions.cfm